Research Article | Vol. 11, No. 4 / 1 April 2020 / *Biomedical Optics Express* 1725

Biomedical Optics EXPRESS

Prefrontal functional connectivity analysis of cognitive decline for early diagnosis of mild cognitive impairment: a functional near-infrared spectroscopy study

JIN-WOO YU,[1,5] SUNG-HO LIM,[1,2,5] BOMIN KIM,[1] EUNHO KIM,[1] KYUNGSOO KIM,[2] SUNG KYU PARK,[3] YOUNG SEOK BYUN,[3] JOON SAKONG,[3,4] AND JI-WOONG CHOI[1,2,*]

[1] *Department of Information and Communication Engineering, DGIST, Daegu 42988, South Korea*
[2] *Brain Engineering Convergence Research Center, DGIST, Daegu 42988, South Korea*
[3] *Department of Occupational and Environmental Medicine, Yeungnam University Hospital, Daegu 42988, South Korea*
[4] *Department of Preventive Medicine and Public Health, College of Medicine, Yeungnam University, Daegu 42988, South Korea*
[5] *These authors equally contributed to this work*
[*] *jwchoi@dgist.ac.kr*

Abstract: Cognitive decline (CD) is a major symptom of mild cognitive impairment (MCI). Patients with MCI have an increased likelihood of developing Alzheimer's disease (AD). Although a cure for AD is currently lacking, medication therapies and/or daily training in the early stage can alleviate disease progression and improve patients' quality of life. Accordingly, investigating CD-related biomarkers via brain imaging devices is crucial for early diagnosis. In particular, "portable" brain imaging devices enable frequent diagnostic checks as a routine clinical tool, and therefore increase the possibility of early AD diagnosis. This study aimed to comprehensively investigate functional connectivity (FC) in the prefrontal cortex measured by a portable functional near-infrared spectroscopy (fNIRS) device during a working memory (WM) task known as the delayed matching to sample (DMTS) task. Differences in prefrontal FC between healthy control (HC) (n = 23) and CD groups (n = 23) were examined. Intra-group analysis (one-sample t-test) revealed significantly greater prefrontal FC, especially left- and inter-hemispheric FC, in the CD group than in the HC. These observations could be due to a compensatory mechanism of the prefrontal cortex caused by hippocampal degeneration. Inter-group analysis (unpaired two-sample t-test) revealed significant intergroup differences in left- and inter-hemispheric FC. These attributes may serve as a novel biomarker for early detection of MCI. In addition, our findings imply that portable fNIRS devices covering the prefrontal cortex may be useful for early diagnosis of MCI.

1. Introduction

Alzheimer's disease (AD) is a chronic progressive neurodegenerative brain disease that typically presents as subtle failures in memory that gradually becomes more acute [1]. In recent years, AD has been reported to be the most common cause of dementia, accounting for 60-80% of dementia cases worldwide [2]. Although a cure for AD is currently lacking, medication therapies and/or daily training in the early stage can alleviate disease progression and improve patients' quality of life [3,4]. Accordingly, early diagnosis of AD is of substantial clinical importance as these therapeutic strategies are more effective during the earlier stages of AD.

Mild cognitive impairment (MCI) is considered to be an intermediate state of cognitive impairment between normal aging and AD [5–7]. Although they do not meet the clinical criteria

#382197
Journal © 2020

https://doi.org/10.1364/BOE.382197
Received 1 Nov 2019; revised 16 Feb 2020; accepted 18 Feb 2020; published 2 Mar 2020

Biomedical Optics EXPRESS

for AD [8], patients with MCI are more likely to develop AD [9]. As such, there is an urgent need to develop approaches for the identification of individuals before or during the earliest stages of AD, with the hope that the intervention could delay or even prevent the onset of clinical symptoms [8]. However, as AD pathology is suspected to begin long before symptoms manifest, it is difficult to diagnose the disease at earlier stages [10]. Accordingly, researchers have focused on the major symptoms of MCI.

The predominant cognitive decline (CD) of MCI is related to thinking, judgment, and memory function. In particular, dysfunction in working memory (WM), which is characterized by impaired reasoning and decision-making, is one of the earliest and most devastating symptoms of MCI [11–13]. Human brain studies have demonstrated that the prefrontal region plays a key role in WM processing [14]. Therefore, prefrontal functional changes during WM processing are likely to be important for understanding the underpinnings of impaired memory function in MCI.

Functional neuroimaging studies have demonstrated abnormal activation in the prefrontal cortices during WM tasks in MCI patients [15,16]. However, the processes related to cognitive function are not isolated to specific brain regions. Rather, these processes result from highly interconnected neural circuits encompassing remote brain regions [13]. Therefore, it is important to explore the functional connections among prefrontal neural circuits related to WM function in order to better understand how they differ between MCI patients and normal participants.

Functional connectivity (FC) analysis is a technique for the *in vivo* examination of cooperating brain regions during a task (or at rest) [17,18]. In task states, the FC of AD patients exhibited different characteristics to that of healthy controls (HCs) in the prefrontal cortex, suggesting that memory dysfunction is related to these changes, based on positron emission tomography (PET) imaging during a face memory task [13]. Electroencephalography (EEG) can be employed to explore dynamic and regional FC alterations in patients with mild AD during a digit verbal span task (DVST) [19]. Previous work has investigated the resting-state FC of AD [20] (or MCI [21]) patients using functional magnetic resonance imaging (fMRI). However, PET and fMRI are technically complex and costly, which limits their use as routine clinical tools.

To address this problem, functional near-infrared spectroscopy (fNIRS) has been used as an alternative modality [15,19,22]. fNIRS uses near-infrared rays (within the 700-900 nm spectral interval) to monitor brain activity by measuring hemodynamic responses related to neuronal behavior, which is based on the principle of neuro-vascular coupling [23,24]. Neuro-vascular coupling refers to the mechanism that links neuronal activity to related changes in localized cerebral blood flow. By transmitting light in the source and receiving reflected and scattered light in the detector (see Fig. 2(B)), the fNIRS device can distinguish oxy- and deoxy-hemoglobin changes according to the degree of absorption of near-infrared light in hemoglobin.

fNIRS offers multiple benefits over PET and fMRI. It features high portability, lower cost, lower susceptibility to movement artifacts, lack of ionizing radiation, and poses fewer constraints to participants during the measurement [25]. Conversely, there are several drawbacks of fNIRS. First, fNIRS is unable to monitor subcortical activity. Nevertheless, it is sufficient to measure major FC as cortical regions (gray matter) consist mainly of somata that generate neural activity during both resting-state measurements [26] and under mental task conditions [27]. Second, fNIRS has lower spatial resolution than that of PET and fMRI. As fNIRS has higher specifications than fMRI and PET with respect to temporal resolution, these techniques are complementary. EEG/magnetoencephalography (MEG) provides higher temporal resolution than that of fNIRS, whereas fNIRS provides higher spatial resolution than that of EEG/MEG. Consequently, fNIRS offers a good trade-off between temporal and spatial resolutions, enabling FC measurement and brain region analysis together. These characteristics make fNIRS a potential alternative technique to PET, fMRI, and EEG/MEG for convenient and non-invasive diagnosis or therapeutic monitoring in routine clinical practice. Accordingly, the use of portable fNIRS devices can reduce the burden of current diagnosis procedures with respect to time, safety, and cost, ultimately

Biomedical Optics EXPRESS

facilitating frequent medical examination and maximizing the efficacy of potential therapies for MCI (or AD).

For this reason, there have been several studies on prefrontal FC analysis using fNIRS to identify typical brain networks of individuals with MCI (or AD). [22] presented a FC analysis of the prefrontal cortex during a semantic verbal fluency task (SVFT) for normal aging, MCI, and AD groups. Although significant differences were observed among groups, it was challenging to identify dysfunction in WM through SVFT. To overcome this limitation, [15] performed a FC analysis of the prefrontal cortex in various tasks including a WM task, and compared inter- and intra-hemispheric connectivity in HC and MCI groups. However, the fNIRS device used in that study only had four channels, which were insufficient to cover the entire prefrontal cortex area and analyze FC with high spatial resolution. Further, no significant differences were observed between HC and MCI groups in the WM task. To the best of our knowledge, there have been no fNIRS studies on WM task-related FC in the prefrontal cortex of participants with CD to date. For early diagnosis of MCI, it is critical to analyze prefrontal FC in elderly individuals with CD to find CD-related biomarkers.

In this study, we measured and analyzed the prefrontal FC of HC and CD participants during a WM task using a portable fNIRS device covering only the prefrontal cortex with four-fold higher spatial resolution than that of other fNIRS devices. We observed that the CD group had greater FC than that of HCs in the prefrontal cortex. In particular, unlike the HC group, greater FC traversing the left and right hemispheres, termed inter-hemispheric FC, was observed in the CD group than in the HC group, with significant differences in FC observed between HC and CD groups. These observations may be due to compensatory mechanisms caused by hippocampal degeneration [28–32]. Based on our findings, we propose that prefrontal FC may be a biomarker for early diagnosis of MCI, and portable fNIRS can be employed as a routine clinical tool for diagnostic assessment of MCI. Furthermore, our findings may facilitate the examination of the pathological mechanisms underpinning MCI leading to AD.

2. Material and methods

2.1. Participants

In this study, we recruited 46 male and female right-handed participants aged from 50-72 years old who were Korean speakers. A neurologist with more than 20 years of experience at the Department of Neurology at Yeungnam University Medical Center (Daegu, South Korea) conducted medical examinations by face-to-face interviews and confirmed that none of the participants had brain, cardiovascular diseases and/or mental disorders. Participants did not report any complaints of subjective symptoms and fell within normal ranges for various medical tests. We also examined participants using the mini-mental state examination (MMSE), a standardized measurement of cognitive state. We categorized participants whose MMSE scores were below 27 points as the CD group. The HC group was organized for the participants whose MMSE scores were above 27 points [33]. All participants were classified into two groups: HC (ages: 61.17 ± 6.45 years, gender: 11 male (M) / 12 female (F), education: 10.45 ± 4.03 years, MMSE score: 29.09 ± 0.73) and CD (ages: 63.17 ± 5.52 years, gender: 10 M/13 F, education: 8.27 ± 3.88 years, MMSE score: 24.74 ± 1.21) groups. No significant differences between the two groups in age (p = 0.261), sex ratio (p = 0.773), or education level (p = 0.075) were observed. A significant difference was noted between groups in MMSE score (p < 0.001). The demographics of each group are listed in Table 1. This study was approved by the DGIST Institutional Review Board (IRB) (approval number: DGIST-190401-HR-007-01). We notified all participants of the purpose, process, and instructions of this experiment. Participants signed a consent form provided by the DGIST IRB before participating in the experiment.

Biomedical Optics EXPRESS

Table 1. Demographics of HC and CD groups.

Characteristic	HC (n = 23)	CD (n = 23)	p-value
Age (years)	61.17 ± 6.45	63.17 ± 5.52	0.261
Gender (M/F)	11M/12F	10M/13F	0.773
Education (years)	10.45 ± 4.03	8.27 ± 3.88	0.075
MMSE (score)	29.09 ± 0.73	24.74 ± 1.21	< 0.001

2.2. Experimental procedure

The experiment was conducted in a quiet room. Each participant sat on a comfortable chair in front of a monitor presenting experimental visual stimuli. Before the experiment, all participants were instructed to maintain their head position still and fixate on the monitor screen. During the experiment, all participants fixated on the screen to perform the delayed matching to sample (DMTS) task. fNIRS data were acquired while participants performed the task.

Before measuring fNIRS signals, an introduction and exercises for the DMTS task were preceded to ensure participants fully understood the task. After the introduction and exercises, each participant performed two DMTS task sessions. Each session consisted of three trials. Trials consisted of encoding, maintenance, retrieval, and rest phases (see Fig. 1). In the encoding phase, participants were presented with a non-verbal visual stimulus for 10 seconds. The stimulus was randomly selected from a certain image set from the Benton visual retention test. The set consisted of four figures with similar geometric shapes; 10 sets of figures were prepared for the experiment. Participants were instructed to memorize the image until they were asked to identify it in the retrieval phase. In the maintenance phase, participants were asked to maintain memory of the image presented in the encoding phase, while staring at a ‘cross sign (+)’ presented in the center of the screen. The phase lasted until the trials’ common delay time (5 s or 15 s) ended. In the retrieval phase, participants were instructed to identify the image that was presented at the encoding phase among four sample images. They answered by indicating an answer image on the touch screen using a finger. In the final step of the trial (a 12-sec rest phase), all participants fixated on the ‘cross sign (+)’ on the screen as instructed beforehand. Response time and performance accuracy of all participants were recorded for data analysis.

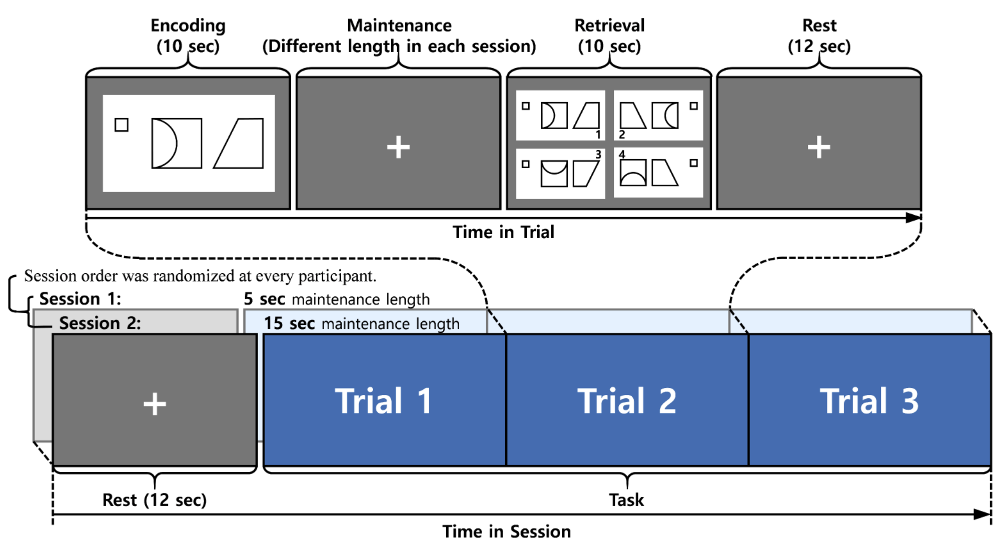

Fig. 1. DMTS task-based experiment protocol.

Biomedical Optics EXPRESS

2.3. fNIRS device

A portable fNIRS device (NIRSIT, OBELAB, Seoul, South Korea) specialized to monitor the prefrontal cortex was used to measure the hemodynamic response. The fNIRS probes were firmly attached on the participants' foreheads using a garment strap placed on the back of the fNIRS device (Fig. 2(A)). NIRSIT is a continuous wave fNIRS device composed of 24 sources, using 780 nm and 850 nm wavelength light, and 32 detectors recording signals at an 8.138 Hz sampling rate. The device provides multi-depth channels with 1.5 cm and 3 cm distances between the source and detector (see Fig. 2(B)). As shown in Fig. 2(B), the measurable depth of the fNIRS device is greater when the distance between the source and detector becomes larger. We selected two types of channel configurations according to source-detector-distance (SDD): 1.5cm and 3cm, avoiding less then 1cm SDD used for the regression to remove the effect of skin and bone blood flow [34,35]. Channel configurations of 1.5 cm and 3 cm for this fNIRS device are shown in Fig. 2(C). The total numbers of 1.5 cm and 3 cm-channels were 52 and 68, respectively. Due to the signal processing technique applied to the device, channels that share an source or detector can measure signals simultaneously. The localization was based on FPz using a 10-10 system. The reference position of the international 10-10 system and estimated Brodmann areas (BAs) are presented in Fig. 2(C).

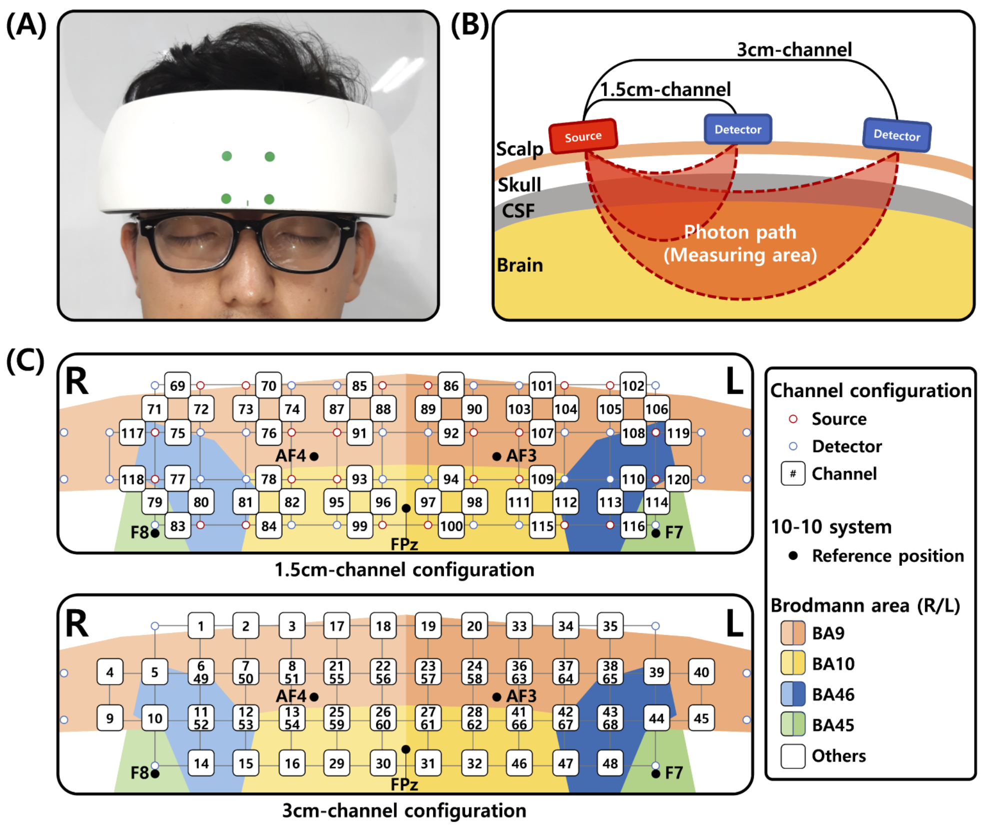

Fig. 2. Experimental setup of the fNIRS device. (A) The fNIRS device placed on a participant's forehead. (B) A schematic diagram of 1.5 cm- and 3 cm-channels in the fNIRS device. (C) 1.5 cm- and 3 cm-channel configurations of the fNIRS device. Each grid size is 15×15 mm. The sources and detectors that overlap with the channel-number notation are not presented.

2.4. Data preprocessing

The measured fNIRS signal, change in optical density, was converted to relative changes in oxygenated hemoglobin (oxy-Hb/HbO) concentration (ΔHbO) via the modified Beer-Lambert law [36]. The channel's signal-to-noise power ratio (SNR) was calculated using the power of optical density signal and noise. Channels with a low SNR (<20 dB) were rejected before extraction of hemodynamic data. The ΔHbO signals were band-pass filtered by a fourth order zero-phase infinite impulse response (IIR) filter (0.009-0.08 Hz) to minimize various artifacts and physiological noise. The cut-off frequencies were set to reject global drifts (<0.009 Hz), Mayer wave (~0.1 Hz), respiration rate (>0.2 Hz), and cardiac cycles (>0.5 Hz). Among filtered ΔHbO signals, we only used the signal derived from a correctly answered task as we considered it evidence of successful recall.

2.5. FC analysis

To measure FC, we used the pre-processed signals of two channels in the retrieval phase of the DMTS task instead of "Encoding" (Fig. 3(A)), as it was possible to determine whether participants attempted to retrieve their memory only by considering "Correct" trials. By considering hemodynamic delay, an additional 2 seconds from the end of the retrieval phase were also used in the calculation. For example, for a specific participant, we first selected "Correct" trials of time-series hemodynamic signals in the retrieval phase among six trials to strictly reflect task-related responses, and then Pearson correlation coefficients (r) between the i-th and j-th channels were calculated as follows:

$$r = \rho\left(\mathbf{y}_i, \mathbf{y}_j\right) = \frac{\sum_{a=1}^{n}\left(y_{i,a}-\bar{y}_i\right)\left(y_{j,a}-\bar{y}_j\right)}{\sqrt{\sum_{a=1}^{n}\left(y_{i,a}-\bar{y}_i\right)^2}\sqrt{\sum_{a=1}^{n}\left(y_{j,a}-\bar{y}_j\right)^2}} \tag{1}$$

where $\rho(\cdot)$ denotes Pearson's correlation, $\mathbf{y}_i(=[y_{i,1}, y_{i,2}, \ldots, y_{i,n}])$ is an n-point time series of i-th channel, $\bar{y}_i$ is the mean of $\mathbf{y}_i$, $\mathbf{y}_j\left(=\left[y_{j,1}, y_{j,2}, \ldots, y_{j,n}\right]\right)$ is an n-point time series of j-th channel, and $\bar{y}_j$ is the mean of $\mathbf{y}_j$. The total number of r calculated as FC in the 1.5 cm- and 3 cm-channel configurations was 1,326 and 2,278, respectively. The total number of r calculated as FC between 1.5 cm- and 3 cm-channels was 3,536. Derived correlation matrices were averaged to reduce the noise effect (Fig. 3(A)). In Fig. 3(C), to change the correlation coefficient r into a normal distribution (z) for the statistical test [37], Fisher transformation, F, was applied as follows:

$$z = F(r) = \frac{1}{2}\ln\frac{1+r}{1-r} \tag{2}$$

In Fig. 3(C), to identify meaningful FC in each group, we used two criteria: average correlation coefficient ($r \geq 0.7$) and statistical significance ($p \leq 0.05$). The average correlation coefficient was computed by averaging all correlation matrices of participants included in the HC (or CD) group in order to investigate the general strength of FC in each group. For the intra-group analysis, the statistical significance of FC in each group was evaluated using a one-sample t-test. This analysis facilitates our understanding of how the tendency of prefrontal FC is altered between HC and CD. In addition, for the inter-group analysis, statistically significant differences of FC between groups were evaluated using an unpaired two-sample t-test.

FC based on the region of interest (ROI) selectively demonstrated FC related to channels showing a significant hemodynamic response during tasks. For the ROI-based FC analysis, we selected ROIs by the slope of time-series signals of the hemodynamic response recorded in the prefrontal cortex (see Fig. 3(B)). For calculating the slope, every ΔHbO signal from the start time (t_0) of the retrieval phase to the peak (or nadirs) (t_p) was linearly regressed according to the equation in Fig. 3(B). Based on a one-sample t-test of the slope values calculated in each group, we selected significant ($p \leq 0.05$) channels with a positive slope value as ROIs [10].

Biomedical Optics EXPRESS

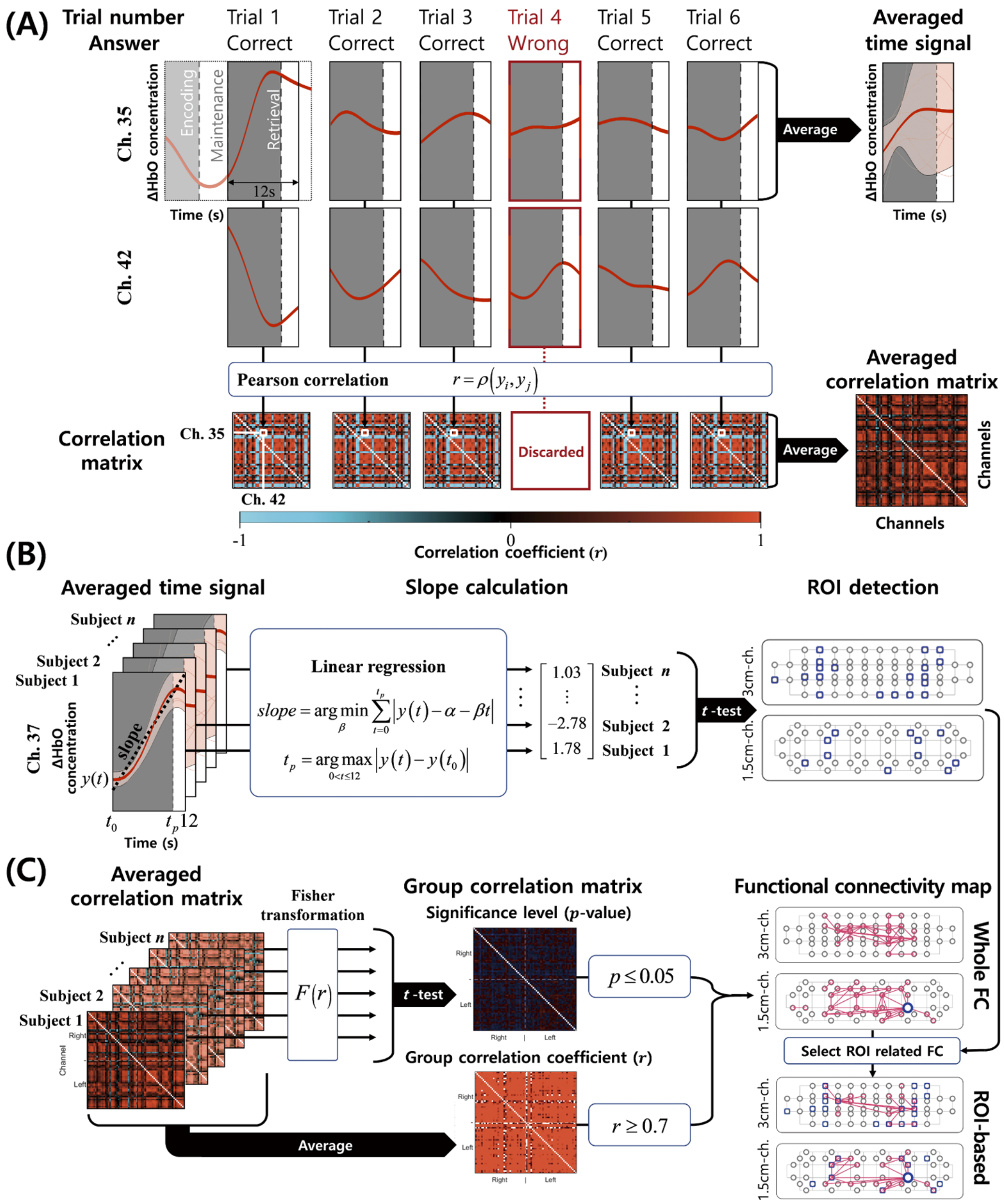

Fig. 3. Explanation of data processing. (A) Averaged time-series signal and correlation matrix of the retrieval phase. (B) ROI detection by selecting channels with a statistically significant ($p \leq 0.05$) slope of the averaged time-series signal. The slope was calculated by linear regression in each participant, and a one-sample t-test was applied to assess statistical significance. (C) Derivation of FC map. Fisher transformation was applied to the averaged correlation matrix of each participant for the statistical significance level based on a t-test ($p \leq 0.05$). By averaging the correlation matrices of all participants, the group correlation coefficient with $r \geq 0.7$ was calculated. Based on the significance level and group correlation coefficient, whole and ROI-based FC maps were derived.

3. Results

3.1. Behavioral results

In order to analyze the WM performance of the HC and CD groups, we measured the accuracy and response time in the retrieval phase of the DMTS task (see Fig. 4). In particular, in Figs. 4(B) and (D), we measured the accuracy and response time according to two maintenance times (5s and 15s), respectively, while Figs. 4(A) and (C) show the overall performance without distinguishing maintenance times.

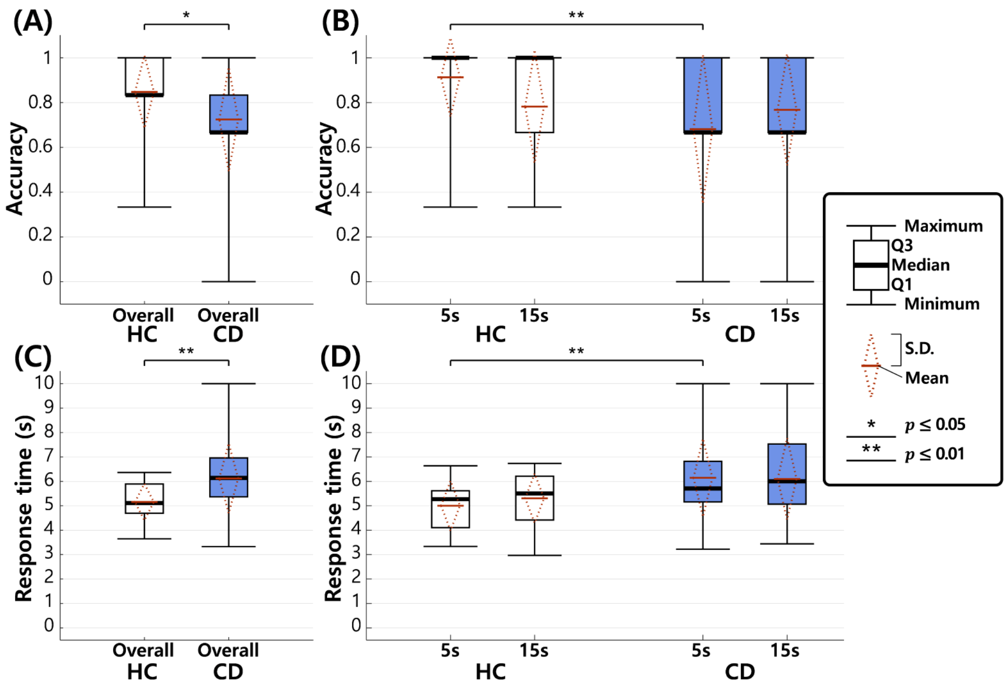

Fig. 4. Behavioral results for accuracy and response time in HC and CD groups. In the legend, Q1 (first quartile) indicates the 25-th percentile, and Q3 (third quartile) indicates the 75-th percentile. In this figure, diamond plots described by a dotted red line indicate standard deviation (S.D.), and the mean value of the corresponding box plots. (A) Overall accuracy. (B) Accuracy according to different maintenance times (5 s and 15 s). (C) Overall response time. (D) Response time according to different maintenance times.

The accuracy of each group was calculated by dividing the number of correctly answered trials by the total number of trials in the DMTS task. For example, the total number of trials in the HC group was calculated as 138 (=23 (number of participants in the HC group) × 2 (number of sessions) × 3 (number of trials in each session)). In Fig. 4(A), the average overall accuracy of the HC group was 84.8% and that of the CD group was 72.5%. We observed that the average overall accuracy was approximately 12.3% points higher in the HC group than in the CD on average. Because the accuracy values are not normally distributed (Shapiro-Wilk test), we applied the Wilcoxon rank sum and Friedman tests. Without distinguishing two maintenance times (5s and 15s), there was a statistically significant difference (p = 0.048, Wilcoxon rank sum test) between the two groups (see Fig. 4(A)). In each maintenance time, a significant difference was observed between the two groups from “5s” (p = 0.006, Wilcoxon rank sum test), while no significant difference (p = 0.819, Wilcoxon rank sum test) was observed from “15s” (see Fig. 4(B)). Also, no

Biomedical Optics EXPRESS

significant difference was observed between different maintenance times (p = 0.449, Friedman test).

The response time was measured from the start time of the retrieval phase (see Fig. 1) until the answer time. The response time in each group was evaluated by averaging the response times of all trials. The response times of non-answered trials were considered as the maximum value (10 seconds), which is the length of the retrieval phase. In Fig. 4(C), we observed that the response time was approximately 0.97 s faster on average in the HC group than in the CD group. Because the response times are normally distributed (Shapiro-Wilk test), we applied an unpaired two-sample t-test and two-way ANOVA. We used Levene's test to test the similarity of variances, and corrected the unequal variances in the statistical test. Without distinguishing two maintenance times (5s and 15s), we found a statistically significant difference (p = 0.008, unpaired two-sample t-test) between the two groups (see Fig. 4(C)). In each maintenance time, a significant difference was observed between the two groups from "5s" (p = 0.007, unpaired two-sample t-test), while no significant difference (p = 0.066, unpaired two-sample t-test) was observed from "15s" (see Fig. 4(D)). Also, no significant difference was observed between different maintenance times (F = 0.196, p = 0.659, two-way ANOVA). The interaction of group × maintenance time was not significant (F = 0.366, p = 0.547, two-way ANOVA).

3.2. WM-related hemodynamic responses of HC and CD groups

Because there have been many researches on the appropriate SDD of fNIRS [34,35,38–41], it is necessary to justify that the main signal contributor in the 1.5cm- and 3cm-channel configurations is not the skin, i.e., that the signal recorded by these channels actually represents brain/neural activity. According to the experimental procedure (see Fig. 1), we measured WM-related hemodynamic responses of the prefrontal cortices of HC and CD groups. We averaged those signals, measured in the retrieval phase of the DMTS task, over trials, channels, and participants. Figure 5 shows those avaraged signals of HC and CD groups. The signals of the 1.5cm-channel configuration increase from the start of the retrieval phase to the end like ones of the 3cm-channel configuration. It means that the signals measured in 1.5cm- and 3cm-channel configuration is task-related (i.e., WM-related). Therefore, we found that the 1.5cm-channel configuration could measure brain/neural activity as well as the 3cm-channel configuration. In a comparison between HC and CD groups, we also found that ΔHbO of the CD group was higher than that of the HC. In case of all channels, ΔHbO of the CD group (ΔHbO = 0.207μM (see Fig. 5(D))) was 0.033μM higher than that of the HC (ΔHbO = 0.174μM (see Fig. 5(A))). In case of the 3cm-channel configuration, ΔHbO of the CD group (ΔHbO = 0.2μM (see Fig. 5(E))) was 0.022μM higher than that of the HC (ΔHbO = 0.178μM (see Fig. 5(B))). In case of the 1.5cm-channel configuration, ΔHbO of the CD group (ΔHbO = 0.219μM (see Fig. 5(F))) was 0.05μM higher than that of the HC (ΔHbO = 0.169μM (see Fig. 5(C))). It means that the CD group had more workload than the HC during the same task.

3.3. FC results

As explained in "FC Analysis", whole and ROI-based FC in the prefrontal cortex during the retrieval phase of the DMTS task were measured, as shown in Fig. 6 and Fig. 7, respectively. First, in the case of whole FC analysis, a one-sample t-test was applied to assess statistically significant ($p \leq 0.05$, $r \geq 0.7$) FC in each group (see Figs. 6(A), B, D, and E). We investigated FC between different channels in each configuration (3 cm- and 1.5 cm-channels) and across different configurations. FC was described as lines between channels, and their colors represent the p-value (see Figs. 6(A) and (B)) and correlation coefficient (see Figs. 6(D) and (E)). In Figs. 6(A) and (B), yellow ($0.01 < p \leq 0.05$), orange ($0.001 < p \leq 0.01$), and red ($p \leq 0.001$) represent the p-values. In Figs. 6(D) and (E), gradational colors from yellowish green (r = 0.7) to red (r = 0.85) were used to represent the correlation coefficients.

Biomedical Optics EXPRESS

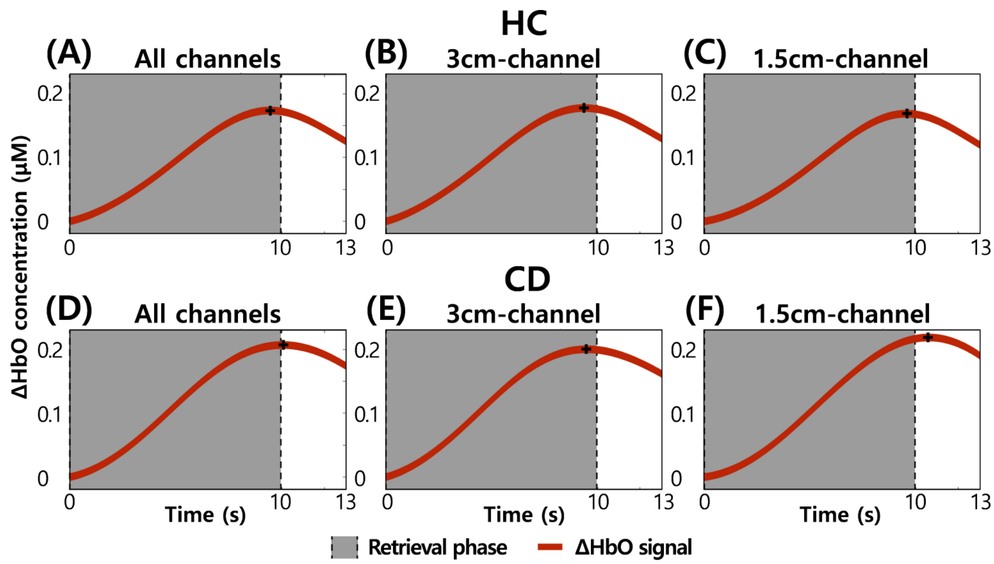

Fig. 5. WM-related prefrontal hemodynamic signals averaged over trials, channels, and participants. (A) The signal averaged over all channels of the HC group. (B) The signal averaged over 3cm-channel of the HC group. (C) The signal averaged over 1.5cm-channel of the HC group. (D) The signal averaged over all channels of the CD group. (E) The signal averaged over 3cm-channel of the CD group. (F) The signal averaged over 1.5cm-channel of the CD group.

Most significant FC with $r \geq 0.7$ had high significance ($p \leq 0.001$; Figs. 6(A) and (B)). The resulted p-values were corrected by the Bonferroni's method. There was a greater number of FC with large r in the CD group than in the HC group (Figs. 6(D) and (E)). Generally, most FC-related channels were present close to AF3 and AF4, as described in Fig. 2(C). Table 2 shows the number of FC in each group according to regions of the prefrontal cortex, based on Fig. 6. Generally, we detected a larger number of FC in the prefrontal cortex of the CD group than in the HC group, which resulted from an increase in left and inter-hemispheric FC in the CD group. In Figs. 6(A), B, D, and E, the core-hub, which refers to the channel with the largest number of FC, is indicated as a channel boldly circled in blue. The core-hub was observed in the same channel (No. 109 channel in the 1.5 cm-channel placement of Fig. 2(C)) in the two groups. The number of FC connected with the core-hub was 16 and 26 in the HC and CD groups, respectively.

Table 2. Number of functional connections in each group.

Types of FC		HC				CD				Significant difference			
		Total	3 cm	1.5 cm	Cross	Total	3 cm	1.5 cm	Cross	Total	3 cm	1.5 cm	Cross
Intra-hemispheric FC	Left	66	20	20	26	99	33	27	39	8	2	4	2
	Right	50	13	18	19	52	13	18	21	2	0	1	1
Inter-hemispheric FC		23	7	8	8	86	20	33	33	4	0	2	2
Total FC		139	40	46	53	237	66	78	93	14	2	7	5

To identify significantly different FC between the two groups, an unpaired two-sample t-test was applied. In Fig. 6(C), FC with a significant difference ($p \leq 0.05$, uncorrected) between the HC and CD groups is represented by lines between channels; the colors represent the p-value (see Fig. 6(C)) and difference in correlation coefficients between the two groups (see Fig. 6(F)). In

Biomedical Optics EXPRESS

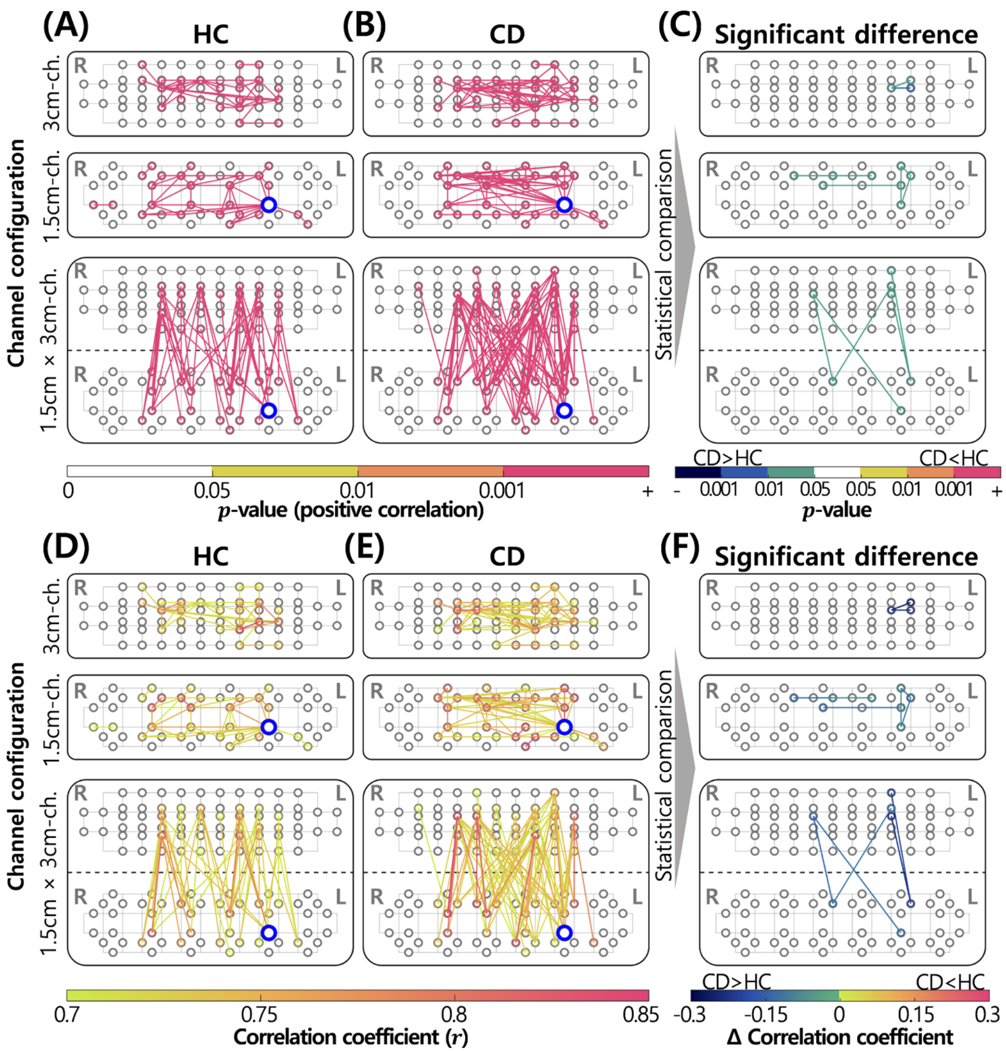

Fig. 6. FC analysis of HC and CD groups. Items circled in gray denote channels. Channels boldly circled in blue represent core-hubs. FC between near channels (≤0.75 cm) is not displayed. (A) Statistically significant FC of the HC group ($p \leq 0.05$). (B) Statistically significant FC in the CD group ($p \leq 0.05$). (C) FC with significant differences between groups ($p \leq 0.05$, uncorrected). (D) Correlation coefficient of statistically significant FC in the HC group ($r \geq 0.7$). (E) Correlation coefficient of statistically significant FC in the CD group ($r \geq 0.7$). (F) Differences in correlation coefficients with statistically significant differences between groups ($p \leq 0.05$, uncorrected).

Biomedical Optics EXPRESS

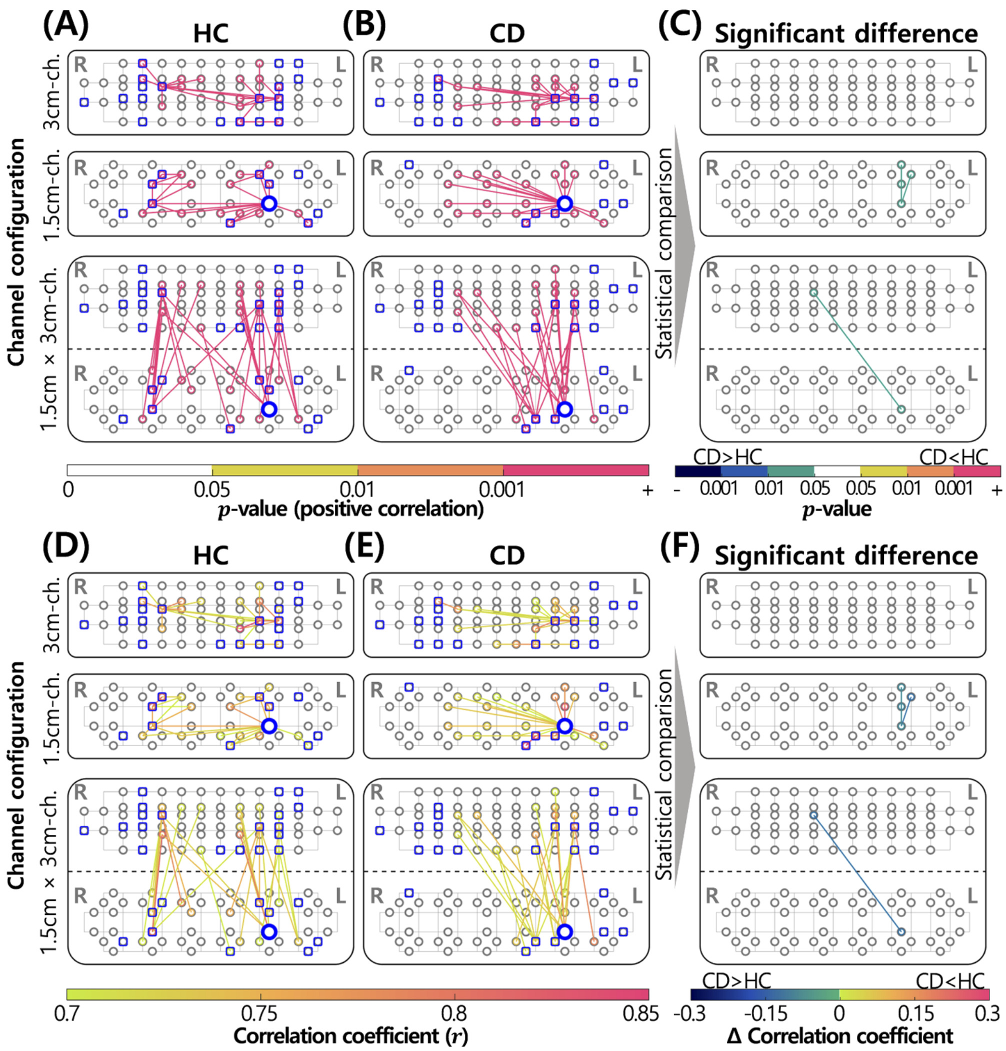

Fig. 7. ROI-based FC analysis of HC and CD groups. Items circled in gray indicate channels. Channels boldly circled in blue indicate core-hubs. Channels selected as ROIs are represented as squares overlapping with gray circles. FC between near channels (≤0.75 cm) is not displayed. (A) Statistically significant ROI-related FC in the HC group ($p \leq 0.05$). (B) Statistically significant ROI-related FC of the CD group ($p \leq 0.05$). (C) ROI-related FC with statistically significant differences between groups ($p \leq 0.05$, uncorrected). (D) Correlation coefficient of statistically significant ROI-related FC in the HC group ($r \geq 0.7$). (E) Correlation coefficient of statistically significant ROI-related FC in the CD group ($r \geq 0.7$). (F) Differences in correlation coefficients with statistically significant differences between groups ($p \leq 0.05$, uncorrected).

Fig. 6(C), green ($0.01<p\leq 0.05$), blue ($0.001<p\leq 0.01$), and dark blue ($p\leq 0.001$) were used when the correlation coefficient was larger in the CD group than in the HC group (CD>HC). Yellow, orange, and red were used when the correlation coefficient was smaller in the CD group than in the HC group (CD<HC). In Fig. 6(F), gradational colors from dark blue to green ($-0.3\leq \Delta r<0$) were used when CD > HC. Colors from yellowish green to red ($0<\Delta r\leq 0.3$) were used when CD < HC. As shown in Figs. 6(C) and (F), FC with the significant difference between two groups was significantly stronger in the CD group than in the HC. Most of them were left- and inter-hemispheric FC (see Table 2). In the 3 cm-channel configuration, only left-hemispheric FC was present, unlike in other channel configurations.

In ROI-based FC analysis (Fig. 7), square-shaped markers that overlapped with the channel configuration are expressed as ROIs. ROI channels, which represent channels where task-induced activation occurred with statistical significance ($p\leq 0.05$, uncorrected), were scattered in areas of the prefrontal cortex except the frontal pole, the central area of BA9 and BA10, as shown in Fig. 2(C). Generally, there was a slightly larger number of ROIs in the left hemisphere of the prefrontal cortex than in the right hemisphere. Similar to the data presented in Fig. 6, we observed a larger number of inter-hemispheric FC in the CD group than in the HC (see Table 3). Although a slightly larger number of left-hemispheric FC was identified in the CD group than in the HC group, we focused on the ratio of left- to right-hemispheric FC in the CD group, which was caused by a significant reduction in FC in right-hemispheric FC. Notably, we observed that the core-hub, which was identified in the whole FC analysis (see Figs. 7(A), B, D, and E), was included in ROIs. This was situated in the left prefrontal cortex in both groups.

Table 3. Number of ROI-related functional connections in each group.

Types of FC		HC				CD				Significant difference			
		Total	3 cm	1.5 cm	Cross	Total	3 cm	1.5 cm	Cross	Total	3 cm	1.5 cm	Cross
Intra-hemispheric FC	Left	41	11	15	15	45	15	14	16	3	0	3	0
	Right	25	6	9	10	1	1	0	0	0	0	0	0
Inter-hemispheric FC		10	3	3	4	20	5	9	6	1	0	0	1
Total FC		76	20	27	29	66	21	23	22	4	0	3	1

An unpaired two-sample t-test revealed a small number of differences between the HC and CD groups (see Figs. 7(C) and (F)). Similar to data presented in Fig. 6(C) and (F), all derived FC in the CD group was significantly stronger than that in the HC group. In the 1.5 cm-channel configuration, only left-hemispheric FC was observed, whereas only inter-hemispheric FC was observed in the cross-channel configuration.

4. Discussion

fNIRS is an emerging method capable of tracking and monitoring localized oxy- and deoxy-hemoglobin changes resulting from cerebral activity by using near-infrared ray sources and detectors placed over the scalp [23]. Near-infrared lights emitted from sources are received as the reflected and scattered one at detectors (see Fig. 2(B)). By monitoring the degree of absorption of near-infrared light in hemoglobin, fNIRS can measure oxy- and deoxy-hemoglobin changes related to neuronal behavior, based on the principle of neuro-vascular coupling [24]. If brain activation occurs concurrently in different brain regions, these regions are considered to be functionally connected [42].

The goal of this study was to evaluate prefrontal FC measured by a portable fNIRS device to facilitate routine monitoring and clinical evaluation as a potential biomarker for the early detection of MCI. Our results indicate that prefrontal FC, measured with the fNIRS device while performing a DMTS task, has distinct characteristics between HC and CD groups. Behavioral

Biomedical Optics EXPRESS

results indicated a functional decline in WM in the CD group, who exhibited lower accuracy and longer response times overall compared to those in the HC group. For the 15-s task maintenance time, no statistically significant differences were observed in accuracy or response time between the two groups. As such, distinguishing CD and HC groups based on behavioral results of task difficulty level with a long maintenance time will be difficult. Accordingly, we measured prefrontal FC in both groups and focused on their differences to more closely analyze functional decline in WM in the CD group.

Before discussing the FC analysis, it was necessary to confirm that our recorded hemodynamic signals were indeed task-related. We firstly measured the task-related hemodynamic responses of the prefrontal cortices of HC and CD groups (see Fig. 5). We observed the task-related signals in the retrieval phase, and found that ΔHbO of the CD group was higher than that of the HC on average [43,44]. Also, local FC and ROIs in the dorsolateral prefrontal cortex (BA 9/46) and left anterior middle frontal gyrus (BA 10L/46L) in both groups are related to retrieval activity of WM [45–48]. In addition, numerous reports have demonstrated a relationship between the dorsolateral prefrontal cortex and DMTS task [49–51]. The core-hub observed in the same channel which was placed on the left hemisphere may provide clues as the core-hub was included in ROIs, which are channels with statistically significant hemodynamic responses. Notably, the left prefrontal cortex is a key region required for divided attention tasks [52–56], which are related with WM [57]. This suggests that our recorded hemodynamic signals were related to the DMTS task.

First, our major discovery was that the number and strength of prefrontal FC increased in the CD group compared to that in the HC group during a WM task. This could be due to compensatory mechanisms of the prefrontal cortex induced by hippocampal degeneration. The hippocampus, which plays a major role in memory function [58], exhibits a decrease in volume and altered FC with deterioration in cognitive function [59]. In MCI patients, FC in the prefrontal cortex is strengthened to compensate for the decrease in FC between the hippocampus and prefrontal cortex. Substantial evidence indicates that a decrease in hippocampal volume in MCI patients is related to increased number and strength of FC in the prefrontal cortex [28–32]. In addition, increased FC in the prefrontal cortex has commonly been reported in MCI patients during the resting state [20,60,61].

Second, we observed that the CD group had a larger number of FC and ROIs in the left hemisphere than in the right-hemisphere. In particular, the core-hub, positioned in the left hemisphere, had a higher number of FC in the CD group than in the HC. Several studies have reported a larger hemodynamic response and FC in the left prefrontal cortex than in the right hemisphere [22,32]. [32] reported that compared to HCs, MCI patients exhibited hyper-activation in the left prefrontal cortex. Further, FC within the prefrontal cortex of MCI patients was reported to be left-biased in a verbal fluency test [22].

Hemodynamic responses in the prefrontal cortex as detected by fNIRS differ according to MCI type and cognitive task [16]. However, no significant differences were observed in prefrontal cortical activation between HC and MCI groups during an *N*-back task for WM. FC may be a better option than hemodynamic responses for identifying significant differences in the CD state.

Current methods for diagnosing MCI have the disadvantages of being subjective (MMSE), invasive (blood test), and/or costly (PET, computed tomography, and MRI). In contrast, fNIRS has relatively low cost and provides sufficient information on the cerebral cortex. Hence, it can be used as a novel tool to screen patients at the initial stage. With a portable fNIRS system, we were able to elucidate FC characteristics of CD, which may serve as a novel biomarker for early detection of MCI.

In future studies, we intend to measure prefrontal FC based on the DMTS task in MCI and AD groups, as reported here. In addition, we will consider a DVST [10], which requires participants to remember and retrieve a sequence of digits instead of an image, to enable more thorough investigation of prefrontal FC related to WM. Finally, as fNIRS measurements are influenced by educational background and gender [62], we will also consider intra- and inter-group analyses according to educational background and gender by increasing the sample size.

5. Conclusion

In this study, we measured and analyzed prefrontal FC of HC and CD groups using a portable fNIRS during a WM task. We observed that the CD group had a greater number of FC than that of the HC in the prefrontal cortex. In particular, unlike the HC group, greater inter- and left-hemispheric FC was observed in the CD group compared to that in the HC group, some of which were significantly different between groups during retrieval. This could have arisen due to compensatory mechanisms caused by hippocampal degeneration. We propose that prefrontal FC may serve as a biomarker for early diagnosis of MCI, and portable fNIRS can be employed as a routine clinical tool to enable efficacious diagnosis of MCI.

Funding

National Research Foundation of Korea (2017M3A9G8084463, 2017R1E1A1A01077393, 2019M3C1B8090840).

Disclosures

The authors declare that there are no conflicts of interest related to this article.

References

1. A. Kumar, A. Singh, and E. Ekavali, "A review on Alzheimer's disease pathophysiology and its management: an update," Pharmacol. Rep. **67**(2), 195–203 (2015).
2. A. Alzheimer's, "2015 Alzheimer's disease facts and figures," Alzheimers Dement. **11**(3), 332–384 (2015).
3. N. J. Gates and P. Sachdev, "Is cognitive training an effective treatment for preclinical and early Alzheimer's disease?" J. Alzheimer's Dis. **42**(s4), S551–S559 (2014).
4. J. Folch, D. Petrov, M. Ettcheto, S. Abad, E. Sánchez-López, M. L. García, J. Olloquequi, C. Beas-Zarate, C. Auladell, and A. Camins, "Current research therapeutic strategies for Alzheimer's disease treatment," Neural Plast. **2016**, 1–15 (2016).
5. R. C. Petersen, R. Doody, A. Kurz, R. C. Mohs, J. C. Morris, P. V. Rabins, K. Ritchie, M. Rossor, L. Thal, and B. Winblad, "Current concepts in mild cognitive impairment," Arch. Neurol. **58**(12), 1985–1992 (2001).
6. R. C. Petersen, G. E. Smith, S. C. Waring, R. J. Ivnik, E. G. Tangalos, and E. Kokmen, "Mild cognitive impairment: clinical characterization and outcome," Arch. Neurol. **56**(3), 303–308 (1999).
7. J. C. Morris, M. Storandt, J. P. Miller, D. W. McKeel, J. L. Price, E. H. Rubin, and L. Berg, "Mild cognitive impairment represents early-stage Alzheimer disease," Arch. Neurol. **58**(3), 397–405 (2001).
8. R. C. Petersen, "Early diagnosis of Alzheimer's disease: is MCI too late?" Curr. Alzheimer Res. **6**(4), 324–330 (2009).
9. R. C. Petersen, "Mild cognitive impairment as a diagnostic entity," J. Intern. Med. **256**(3), 183–194 (2004).
10. R. Li, G. Rui, W. Chen, S. Li, P. E. Schulz, and Y. Zhang, "Early detection of Alzheimer's disease using noninvasive near-infrared spectroscopy," Front. Aging Neurosci. **10**, 366 (2018).
11. G. Gainotti, C. Marra, G. Villa, V. Parlato, and F. Chiarotti, "Sensitivity and specificity of some neuropsychological markers of Alzheimer disease," Alzheimer Dis. Assoc. Disord. **12**(3), 152–162 (1998).
12. A. E. Budson and B. H. Price, "Memory dysfunction," N. Engl. J. Med. **352**(7), 692–699 (2005).
13. C. L. Grady, M. L. Furey, P. Pietrini, B. Horwitz, and S. I. Rapoport, "Altered brain functional connectivity and impaired short-term memory in alzheimer's disease," Brain **124**(4), 739–756 (2001).
14. R. Cabeza and L. Nyberg, "Neural bases of learning and memory: functional neuroimaging evidence," Curr. Opin. Neurol. **13**(4), 415–421 (2000).
15. T. Nguyen, M. Kim, J. Gwak, J. J. Lee, K. Y. Choi, K. H. Lee, and J. G. Kim, "Investigation of brain functional connectivity in patients with mild cognitive impairment: A functional near-infrared spectroscopy (FNIRS) study," J. Biophotonics **12**(9), 1–10 (2019).
16. J. A. Yoon, I. J. Kong, J. Choi, J. Y. Baek, E. J. Kim, Y.-I. Shin, M.-H. Ko, Y. B. Shin, and M. J. Shin, "Neural compensatory response during complex cognitive function tasks in mild cognitive impairment: A near-infrared spectroscopy study," Neural Plast. **2019**, 1–8 (2019).
17. K. J. Friston, C. D. Frith, P. Fletcher, P. Liddle, and R. S. Frackowiak, "Functional topography: multidimensional scaling and functional connectivity in the brain," Cereb. Cortex **6**(2), 156–164 (1996).
18. K. Friston, C. Frith, P. Liddle, and R. Frackowiak, "Functional connectivity: the principal-component analysis of large (PET) data sets," J. Cereb. Blood Flow Metab. **13**(1), 5–14 (1993).

19. R. Li, T. Nguyen, T. Potter, and Y. Zhang, "Dynamic cortical connectivity alterations associated with alzheimer's disease: An EEG and FNIRS integration study," NeuroImage: Clin. **21**, 101622 (2019).
20. K. Wang, M. Liang, L. Wang, L. Tian, X. Zhang, K. Li, and T. Jiang, "Altered functional connectivity in early alzheimer's disease: A resting-state fmri study," Hum. Brain Mapp. **28**(10), 967–978 (2007).
21. C.-Y. Wee, S. Yang, P.-T. Yap, D. Shen, and A. D. N. Initiative, "Sparse temporally dynamic resting-state functional connectivity networks for early mci identification," Brain Imaging Behav. **10**(2), 342–356 (2016).
22. T. B. Tang and Y. L. Chan, "Functional connectivity analysis on mild Alzheimer's disease, mild cognitive impairment and normal aging using FNIRS," in *2018 40th Annual International Conference of the IEEE Engineering in Medicine and Biology Society (EMBC)*, (IEEE, 2018), pp. 17–20.
23. M. Ferrari and V. Quaresima, "A brief review on the history of human functional near-infrared spectroscopy (FNIRS) development and fields of application," NeuroImage **63**(2), 921–935 (2012).
24. P. T. Fox and M. E. Raichle, "Focal physiological uncoupling of cerebral blood flow and oxidative metabolism during somatosensory stimulation in human subjects," Proc. Natl. Acad. Sci. **83**(4), 1140–1144 (1986).
25. A.-C. Ehlis, S. Schneider, T. Dresler, and A. J. Fallgatter, "Application of functional near-infrared spectroscopy in psychiatry," NeuroImage **85**, 478–488 (2014).
26. R. C. Mesquita, M. A. Franceschini, and D. A. Boas, "Resting state functional connectivity of the whole head with near-infrared spectroscopy," Biomed. Opt. Express **1**(1), 324–336 (2010).
27. F. S. Racz, P. Mukli, Z. Nagy, and A. Eke, "Increased prefrontal cortex connectivity during cognitive challenge assessed by FNRIS imaging," Biomed. Opt. Express **8**(8), 3842–3855 (2017).
28. T. T. Kircher, S. Weis, K. Freymann, M. Erb, F. Jessen, W. Grodd, R. Heun, and D. T. Leube, "Hippocampal activation in patients with mild cognitive impairment is necessary for successful memory encoding," J. Neurol., Neurosurg. Psychiatry **78**(8), 812–818 (2007).
29. R. Sperling, "Functional mri studies of associative encoding in normal aging, mild cognitive impairment, and Alzheimer's disease," Ann. N. Y. Acad. Sci. **1097**(1), 146–155 (2007).
30. F. Agosta, M. A. Rocca, E. Pagani, M. Absinta, G. Magnani, A. Marcone, M. Falautano, G. Comi, M. L. Gorno-Tempini, and M. Filippi, "Sensorimotor network rewiring in mild cognitive impairment and Alzheimer's disease," Hum. Brain Mapp. **31**, 515–525 (2009).
31. D. Lenzi, L. Serra, R. Perri, P. Pantano, G. Lenzi, E. Paulesu, C. Caltagirone, M. Bozzali, and E. Macaluso, "Single domain amnestic mci: a multiple cognitive domains fmri investigation," Neurobiol. Aging **32**(9), 1542–1557 (2011).
32. F. Clément, S. Gauthier, and S. Belleville, "Executive functions in mild cognitive impairment: emergence and breakdown of neural plasticity," Cortex **49**(5), 1268–1279 (2013).
33. S. N. U. B. Hospital, "Standardization of dementia screening tests," Tech. Rep. 11-1351000-000589, Seoul National University Bundang Hospital (2009).
34. T. Funane, H. Atsumori, T. Katura, A. N. Obata, H. Sato, Y. Tanikawa, E. Okada, and M. Kiguchi, "Quantitative evaluation of deep and shallow tissue layers' contribution to fnirs signal using multi-distance optodes and independent component analysis," NeuroImage **85**, 150–165 (2014).
35. S. Brigadoi and R. J. Cooper, "How short is short? Optimum source–detector distance for short-separation channels in functional near-infrared spectroscopy," Neurophotonics **2**(2), 025005 (2015).
36. D. T. Delpy, M. Cope, P. van der Zee, S. Arridge, S. Wray, and J. Wyatt, "Estimation of optical pathlength through tissue from direct time of flight measurement," Phys. Med. Biol. **33**(12), 1433–1442 (1988).
37. T. Nguyen, O. Babawale, T. Kim, H. J. Jo, H. Liu, and J. G. Kim, "Exploring brain functional connectivity in rest and sleep states: a FNIRS study," Sci. Rep. **8**(1), 16144–10 (2018).
38. E. Okada, M. Firbank, M. Schweiger, S. R. Arridge, M. Cope, and D. T. Delpy, "Theoretical and experimental investigation of near-infrared light propagation in a model of the adult head," Appl. Opt. **36**(1), 21–31 (1997).
39. M. Firbank, E. Okada, and D. T. Delpy, "A theoretical study of the signal contribution of regions of the adult head to near-infrared spectroscopy studies of visual evoked responses," NeuroImage **8**(1), 69–78 (1998).
40. P. Pinti, F. Scholkmann, A. Hamilton, P. Burgess, and I. Tachtsidis, "Current status and issues regarding pre-processing of FNIRS neuroimaging data: an investigation of diverse signal filtering methods within a general linear model framework," Front. Hum. Neurosci. **12**, 505 (2019).
41. L. Gagnon, R. J. Cooper, M. A. Yücel, K. L. Perdue, D. N. Greve, and D. A. Boas, "Short separation channel location impacts the performance of short channel regression in NIRS," NeuroImage **59**(3), 2518–2528 (2012).
42. C.-M. Lu, Y.-J. Zhang, B. B. Biswal, Y.-F. Zang, D.-L. Peng, and C.-Z. Zhu, "Use of FNIRS to assess resting state functional connectivity," J. Neurosci. Methods **186**(2), 242–249 (2010).
43. F. Z. Yetkin, R. N. Rosenberg, M. F. Weiner, P. D. Purdy, and C. M. Cullum, "Fmri of working memory in patients with mild cognitive impairment and probable Alzheimer's disease," Eur. Radiol. **16**(1), 193–206 (2006).
44. R. Heun, K. Freymann, M. Erb, D. T. Leube, F. Jessen, T. T. Kircher, and W. Grodd, "Mild cognitive impairment (MCI) and actual retrieval performance affect cerebral activation in the elderly," Neurobiol. Aging **28**(3), 404–413 (2007).
45. C. Ranganath, M. K. Johnson, and M. D'Esposito, "Prefrontal activity associated with working memory and episodic long-term memory," Neuropsychologia **41**(3), 378–389 (2003).
46. C. Babiloni, A. Ferretti, C. Del Gratta, F. Carducci, F. Vecchio, G. L. Romani, and P. M. Rossini, "Human cortical responses during one-bit delayed-response tasks: an FMRI study," Brain Res. Bull. **65**(5), 383–390 (2005).

Biomedical Optics EXPRESS

47. M. Rugg, P. Fletcher, C. Frith, R. Frackowiak, and R. J. Dolan, "Differential activation of the prefrontal cortex in successful and unsuccessful memory retrieval," Brain **119**(6), 2073–2083 (1996).
48. E. Düzel, T. W. Picton, R. Cabeza, A. P. Yonelinas, H. Scheich, H.-J. Heinze, and E. Tulving, "Comparative electrophysiological and hemodynamic measures of neural activation during memory-retrieval," Hum. Brain Mapp. **13**(2), 104–123 (2001).
49. R. H. Bauer and J. M. Fuster, "Delayed-matching and delayed-response deficit from cooling dorsolateral prefrontal cortex in monkeys," J. Comp. Physiol. Psychol. **90**(3), 293–302 (1976).
50. S. Funahashi, C. J. Bruce, and P. S. Goldman-Rakic, "Dorsolateral prefrontal lesions and oculomotor delayed-response performance: evidence for mnemonic "scotomas"," J. Neurosci. **13**(4), 1479–1497 (1993).
51. T. Sawaguchi and I. Yamane, "Properties of delay-period neuronal activity in the monkey dorsolateral prefrontal cortex during a spatial delayed matching-to-sample task," J. Neurophysiol. **82**(5), 2070–2080 (1999).
52. S. A. Bunge, T. Klingberg, R. B. Jacobsen, and J. D. Gabrieli, "A resource model of the neural basis of executive working memory," Proc. Natl. Acad. Sci. **97**(7), 3573–3578 (2000).
53. A. J. Szameitat, T. Schubert, K. Müller, and D. Y. Von Cramon, "Localization of executive functions in dual-task performance with FMRI," J. Cogn. Neurosci. **14**(8), 1184–1199 (2002).
54. T. Schubert and A. J. Szameitat, "Functional neuroanatomy of interference in overlapping dual tasks: an FMRI study," Cognit. Brain Res. **17**(3), 733–746 (2003).
55. R. Loose, C. Kaufmann, D. P. Auer, and K. W. Lange, "Human prefrontal and sensory cortical activity during divided attention tasks," Hum. Brain Mapp. **18**(4), 249–259 (2003).
56. J. A. Johnson and R. J. Zatorre, "Neural substrates for dividing and focusing attention between simultaneous auditory and visual events," NeuroImage **31**(4), 1673–1681 (2006).
57. V. Santangelo and E. Macaluso, "The contribution of working memory to divided attention," Hum. Brain Mapp. **34**(1), 158–175 (2013).
58. H. Eichenbaum, "Hippocampus: cognitive processes and neural representations that underlie declarative memory," Neuron **44**(1), 109–120 (2004).
59. L. Farràs-Permanyer, J. Guàrdia-Olmos, and M. Peró-Cebollero, "Mild cognitive impairment and FMRI studies of brain functional connectivity: the state of the art," Front. Psychol. **6**, 1095 (2015).
60. Z. Qi, X. Wu, Z. Wang, N. Zhang, H. Dong, L. Yao, and K. Li, "Impairment and compensation coexist in amnestic MCI default mode network," NeuroImage **50**(1), 48–55 (2010).
61. P. Liang, Z. Li, G. Deshpande, Z. Wang, X. Hu, and K. Li, "Altered causal connectivity of resting state brain networks in amnesic mci," PLoS One **9**(3), e88476 (2014).
62. P. Robert, S. Ferris, S. Gauthier, R. Ihl, B. Winblad, and F. Tennigkeit, "Review of Alzheimer's disease scales: is there a need for a new multi-domain scale for therapy evaluation in medical practice?" Alzheimer's Res. Ther. **2**(4), 24 (2010).